Two-Dimensional Metamaterials for Dual-Band Filter Applications

Kai Herbertz[1], Stepan Lucyszyn

Department of Electrical and Electronic Engineering, Imperial College
South Kensington Campus, London, SW7 2AZ, UK

[1]k.herbertz@imperial.ac.uk

Abstract—A new EBG cell has been investigated and employed to create a dual-band filter. The unique aspect of this cell is that only lumped-element behaviour defines the lower pass-band, while its distributed-element characteristics influence the upper pass-band. S-band measurements of a prototype confirm the filter functions as predicted by electromagnetic simulations.

I. Introduction

Electromagnetic (EM) bandgap structures, also referred to as photonic bandgap structures when the frequency of the EM wave is within the optical frequency range, derive their name from an analogy to solid-state electronic bandgap structures. With the latter, there are certain energy levels that electrons can occupy and a forbidden band of energy levels that cannot be occupied. With electromagnetic bandgaps (EBGs), the forbidden band pertains to energy levels that photons cannot occupy. Hence, EM waves with a frequency inside the forbidden band cannot propagate through the EBG material, irrespective of their angle of incidence [1].

The term *metamaterials* encompasses various periodic structures with properties that do not exist in nature. There are several different classes of metamaterials. Engheta and Ziolkowski divided their book on metamaterials into the single- and double-negative material class and the EBG structured metamaterial class [2]. This paper employs the latter class for the demonstration of a new high frequency filter for dual-band applications.

The interest in EBGs surfaced in 1987 [3] and initially concentrated on manipulating the propagation of light. However, since the same principles apply to electromagnetic waves in general, electromagnetic bandgap structures are also considered useful in the microwave- and millimetre-wave regimes as well.

Planar EBGs are of particular interest, due to ease of fabrication. However, these two-dimensional (2D) EBGs are usually merely periodic in a 2D plane and do not exhibit a bandgap for all angles of incidence of an EM wave, but just for all angles in that one plane. Within the group of planar EBGs, the uniplanar compact (UC) EBG [4] was chosen as a starting point. Several other works [5-9] also investigated this type of UC EBG, although with scaled dimensions.

This paper describes the design of a new EBG cell. The viability of creating a metamaterial has been proven by demonstrating a band-pass filter using printed circuit board (PCB) technology.

The Section II describes how the cell and the filter were designed and fabricated. Section III contains the results from electromagnetic and circuit modelling. Section IV discusses the measured results, as well as their interpretation. Section V gives a brief discussion and conclusions.

II. Filter Design

The starting point for the metamaterial filter is the conventional UC-EBG. Figure 1 shows the plan view of a generic UC-EBG cell. Here, coupling between UC-EBG cells is through a series inductor, L_s, in parallel with two series capacitors, C_s. There are no vias and, therefore, this UC-EBG exhibits only a shunt capacitance, C_p, (i.e. without any parallel shunt inductance, L_p).

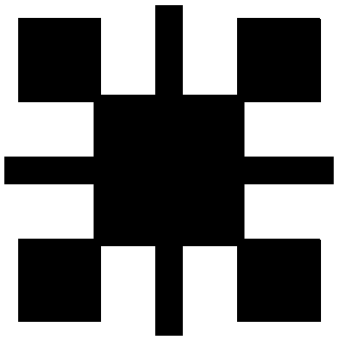

Fig. 1 Plan view of a generic UC-EBG cell [4]

With our approach, the inductors are replaced with much longer high-impedance transmission lines. Figure 2 shows the plan view of the new cell. Moreover, between cells, these meandered lines were short-circuited to ground.

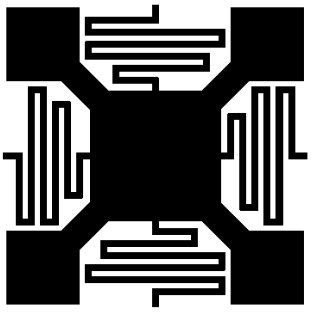

Fig. 2 Plan view of the new EBG cell

The substrate material used for the working prototype was the Taconic RF35 (having $\varepsilon_r = 3.5$, $\tan\delta = 0.0018$ at 1.9 GHz), having a thickness of 250 µm. The copper metallization layer has a thickness of 18 µm, which is also plated with a very thin layer of gold. The resulting physical dimensions for the cell are 1 x 1 cm^2. The length of an edge-coupled series capacitor is 2,400 µm, with a separation distance of 200 µm. The meandered lines have both a track width and gap separation distance of 200 µm.

The filter consists of a 50 Ω microstrip line, embedded between two metamaterial cell arrays. Several filters, having different array sizes were investigated (e.g. 1 cell and 2 x 2 to 6 x 6 cells). In addition, the track widths and spacing were varied with identical 100, 150 and 200 µm values. The filter with 3 x 3 cell arrays on each side of the microstrip line and 200 µm track width and spacing yielded the best roll-off characteristic against minimum passband insertion loss.

III. Simulation Results

A. Electromagnetic Modelling

Figure 3 shows the model setup for HFSS™ simulations of the 3 x 3 metamaterial cell arrays. Since the structure is symmetrical, only one half of the filter has to be computed. The symmetry plane was set up with a perfect-H symmetry boundary, requiring the impedance multiplier to be set to 0.5.

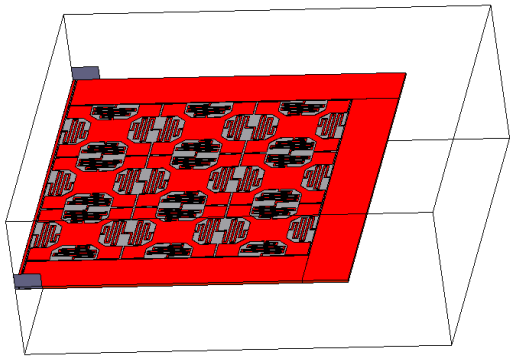

Fig. 3 Model setup for HFSS™ simulations of the 3 x 3 array filter

The predicted HFSS™ simulation results can be seen in Figure 4. The same substrate material properties quoted by the manufacturer, as stated above, were used for the simulations.

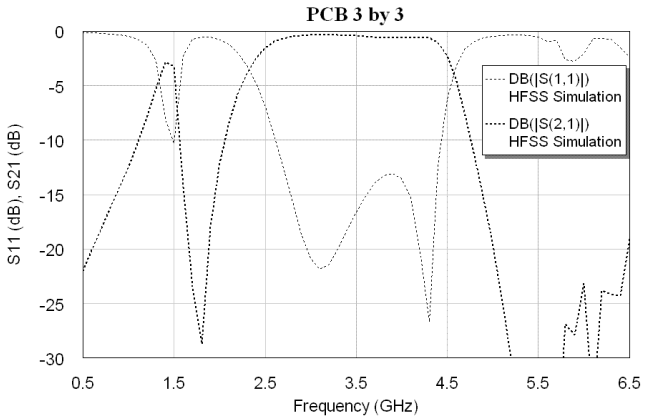

Fig. 4 Predicted simulation results for the 3 x 3 array metamaterials filter

The thick dashed line represents insertion loss and the thin dashed line represents return loss. The filter was designed to have two passbands, which can both be seen in Figure 4.

With the main upper passband only, a very crude attempt was made to compare the effective equivalent filter order with that of a theoretical Butterworth filter approximation. Figure 5 shows the calculated insertion losses for three Butterworth band-pass filter approximations. From these, the 9th-order filter has the best fit. Even though the lower frequency roll-off characteristic is sharper with the calculated Butterworth approximation, the upper frequency roll-off is almost identical to that for the simulated EBG filter.

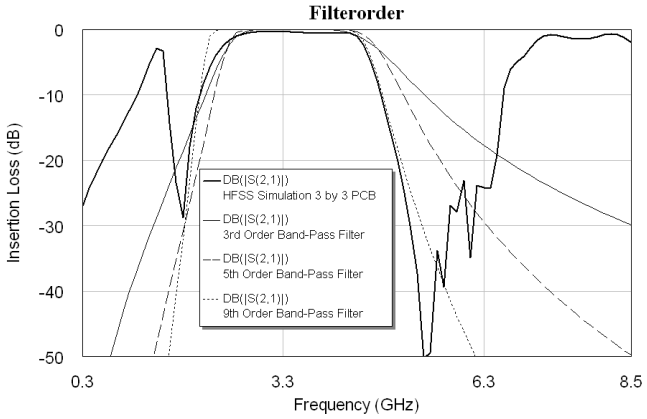

Fig. 5 Estimation of the effective equivalent filter order

B. Circuit Modelling

Circuit modelling (using Microwave Office) was also undertaken, in addition to EM modelling. This approach allows for design changes to be investigated in much shorter times. It also has the added benefit of parameter extraction from measurements (as will be seen in Section IV).

The resonant frequency of the series inductor in parallel with both series capacitors is given by $\omega_s = 1/\sqrt{2L_sC_s}$. With our particular design, the series coupling capacitance between cells is of the order of femtofarads, and so this resonant frequency will be well above the upper passband. Moreover,

since there is little capacitance and no inductance coupling between adjacent cells, it can be concluded that, for this particular design example, a much more compact 3 x 1 array is expected to give the same performance as our 3 x 3 array.

For the frequency range below around 2 GHz, the cells of the first row can be simplified to the equivalent circuit model shown in Figure 6(a).

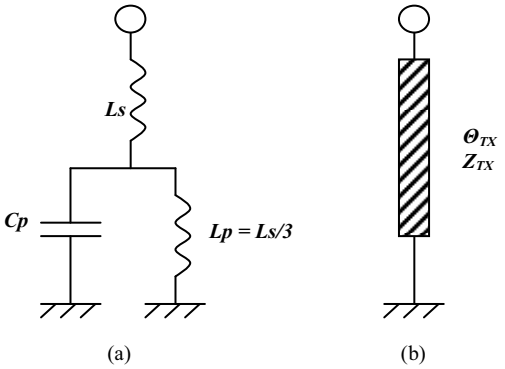

Fig. 6 Equivalent circuit model for a cell in the first row: (a) low frequency; and (b) high frequency

The low frequency driving-point impedance for this cell is given by the following expression:

$$Z(\omega) = j\omega L_s \frac{(4-\omega^2 L_s C_p)}{(3-\omega^2 L_s C_p)}$$

This means that the filter's low frequency lumped-element transmission zeros occur at $\omega_{z1}=0$ and $\omega_{z2} = 2/\sqrt{L_s C_p}$, and transmission pole at $\omega_p = \sqrt{3/L_s C_p}$. Therefore, this pole represents the parallel resonance of the three grounded series inductors with the shunt capacitance of the cell, and defines the lower passband. It is worth noting that the relative spectral positions of the second transmission zero to transmission pole is fixed, since $\omega_{z2}/\omega_p = 2/\sqrt{3} \cong 1.155$ is constant. As a result, while the position of the lower passband and lower EBG can be easily tuned, the ability to control its shape is limited.

The upper passband and upper EBG stem from the transmission line behaviour of the meandered line at higher frequencies. In addition, the shunt capacitance acts as a low impedance connection to ground at high frequencies. As a result, as frequency increases, the meandered lines act as quarter-wave short-circuit stubs and then half-wave short-circuit stubs, etc.; the cell can thus be represented by the stub illustrated in Figure 6(b). With the former, the RF short circuit is transformed into an open circuit. This allows transmission through the filter's microstrip line without impediment, giving rise to the upper passband seen in Figure 4. With the latter, the RF short circuit is transformed back into a short circuit, stopping transmission through the filter's microstrip line, corresponding to the upper EBG in Figure 4. Further harmonic passbands and stopbands will also be evident, due to the three quarter-wavelength stub and full-wavelength stub, etc.

IV. Measurements

Figure 7 shows a photograph of the 3 x 3 array PCB metamaterials filter demonstrator under test.

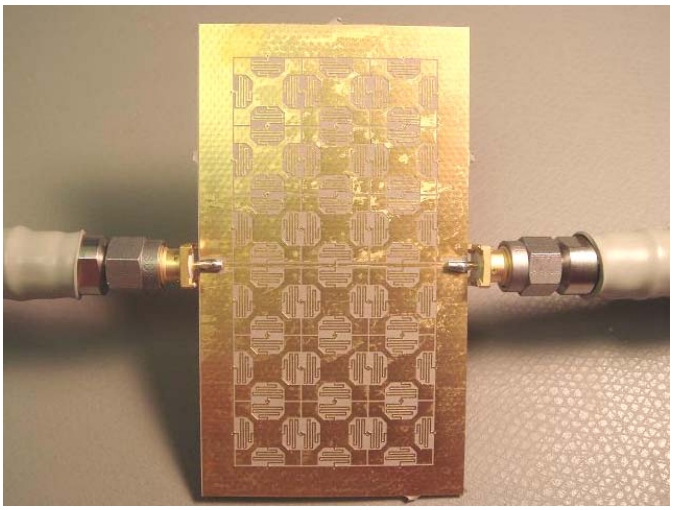

Fig. 7 Photograph of the 3 x 3 array metamaterials filter

Figure 8 shows the measured results for the corresponding filter. The thick continuous line represents the insertion loss and the thin continuous line represents the return loss. There is good agreement between the HFSS™ simulations and the measurements. The centre frequency of the lower passband is 1.18 GHz, having a 3.5 dB insertion loss. The 3 dB passband edges are at 1.04 and 1.29 GHz, having a bandwidth of 0.25 GHz. The centre frequency of the upper passband is 3.4 GHz, having a 1.8 dB insertion loss. The 3 dB passband edges are at 2.26 GHz and 4.53 GHz, having a bandwidth of 2.27 GHz.

Figure 9 compares fitted circuit simulation results with measurements. Within this model, a meandered line is represented by a single straight microstrip line circuit element MLIN. In order to achieve the best fit, the physical length of the meandered line was reduced to 77% (to account for the EM coupling between meanders) and the loss tangent of the substrate was increased from 0.0018 to 0.04 (to account for higher losses). With the Microwave Office simulations, the capacitances were initially calculated using ideal equations based on simple geometry and ignoring fringing fields, giving C_p = 5.53 pF and C_s = 1.9 fF. The circuit simulator then extracted a value of C_p = 5.65 pF to give a better fit to measurements. At the second transmission zero, the extracted inductance value of the meander was found to be L_s = 7.15 nH, with each meander exhibiting an additional shunt capacitance to ground of $C_{p,meander}$ = 300 fF. It was also found that in practice the measurements gave $\omega_{z2}/\omega_p = 1.242$.

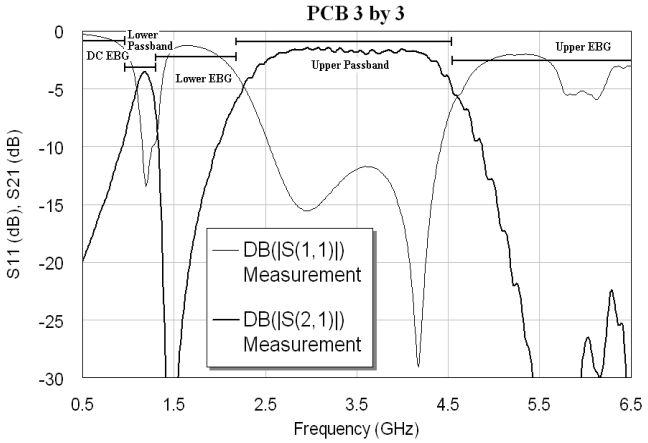

Fig. 8 Measurement results for the 3 x 3 array metamaterials filter

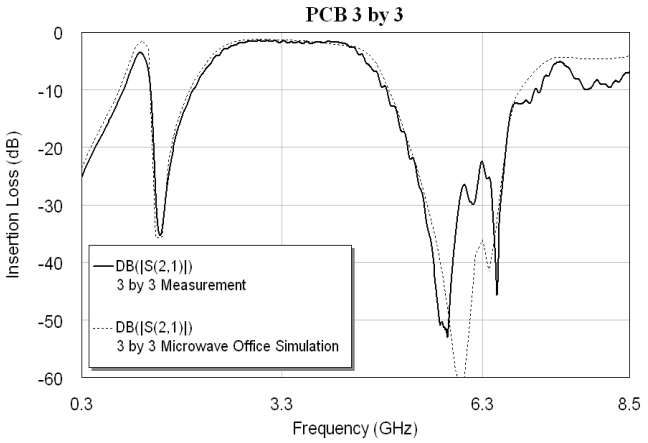

Fig. 9 Comparison of measured and fitted circuit simulation results

V. CONCLUSIONS

The relationship between the number of cells, the minimum insertion loss and roll-off characteristics of the passbands is currently being examined. As the number of cells increases, the roll-off characteristics improve, but the insertion loss also increases. Another aspect that is being investigated is the capacitive coupling between cells. In the design presented here, the capacitive coupling between cells does not affect the low frequency behaviour of the filter.

Directly related to the aim of increasing the capacitance between cells is the introduction of tunability. Ideally, the filter would not be fixed for specific frequency bands, but can be tunable. So far, the tunability of the EBG (e.g. by introducing defects into the lattice) was realised with *p-i-n* and varactor diodes [10]. An obvious approach is to take advantage of the benefits of RF MEMS tunable capacitors, which can in principle provide superior performance when compared to solid-state diodes [11]. Indeed, the meandered lines can double-up as springs, so that the cells can be suspended; not only will this eliminate dielectric losses but allows C_p to be tuned under electrostatic actuation

The aim of this work, to create a dual-band filter using metamaterials, has been demonstrated. The unique aspect of this cell is that only lumped-element behaviour defines the lower pass-band, while its distributed-element characteristics influence the upper pass-band. By tuning specific components of the cell, the lower and upper passbands can be made tunable.

ACKNOWLEDGEMENT

This work is partly funded by the UK's Engineering and Physical Sciences Research Council (EPSRC), under the Platform Grant entitled 'Platform Support for 3D Electrical MEMS' (EP/E063500/1).

REFERENCES

[1] E. Yablonovitch, "Photonic Band-Gap Structures," *Journal Optical Society of America*, vol. 10, no. 2, pp. 283 – 295, Feb. 1993

[2] N. Engheta, R. W. Ziolkowski, *Metamaterials Physics and Engineering Explorations*, 1st ed., John Wiley & Sons, Inc., 2006

[3] E. Yablonovitch, "Inhibited Spontaneous Emission in Solid-State Physics and Electronics," *Physical Review Letters*, vol. 58, no. 20, pp. 2059 – 2062, May 1987

[4] Y. Fei-Ran, M. Kuang-Ping, Q. Yongxi, and T. Itoh, "A uniplanar compact photonic-bandgap (UC-PBG) structure and its applications for microwave circuit," *Microwave Theory and Techniques, IEEE Transactions*, vol. 47, no. 8, pp. 1509 – 1514, Aug. 1999

[5] R. Coccioli, F. R. Yang, K. P. Ma, and T. Itoh, "Aperture-Coupled Patch Antenna on UCPBG substrate," *IEEE Transactions on Microwave Theory and Techniques*, vol. 47, no. 11, pp. 2123 – 2130, Nov. 1999

[6] C. Caloz, C. Chang, Y. Qian, and T. Itoh, "A novel multilayer photonic band-gap (PBG) structure for microstrip circuits and antennas," *Antennas and Propagation Society International Symposium, 2001. IEEE*, vol. 2, pp. 502 – 505, Jul. 2001

[7] P. Meissner, and M. Kitlinski, "Broadside coupled stripline with double-side UC-PBG structure," *Microwaves, Radar and Wireless Communications, 2004. MIKON-2004. 15th International Conference on*, vol. 2, pp. 747 – 750, May 2004

[8] Y. Chen, and C. Tzuang, "Fields and Waves in Microstrip on Uniplanar Compact Photonic-Bandgap (UC-PBG) Ground Plane," *31st European Microwave Conference*, pp. 177 – 180, London 2001

[9] W. Kim, and B. Lee, "Modelling and design of 2D UC-PBG structure using transmission line theory," *Antennas and Propagation Society International Symposium*, 2002. IEEE, vol. 3, pp. 780 – 783, Jun. 2002

[10] M. Belaid, and W. Ke, "Spatial power amplifier using a passive and active TEM waveguide concept," *Microwave Theory and Techniques, IEEE Transactions*, vol. 51, no. 3, pp. 684 – 689, Mar. 2003

[11] S. Lucyszyn, "Review of radio frequency microelectromechanical systems technology," *Science, Measurement and Technology, IEE Proceedings*, vol. 151, issue 2, pp. 93 – 103, Mar. 2004